A CLOUDINESS TRANSITION IN A MARINE BOUNDARY LAYER

Alan K. Betts
RD2, Box 3300
Middlebury, VT   05753
and
Reinout Boers
Code 617, NASA/Goddard Space Flight Center
Greenbelt, MD   20771
June 1989

1)   Introduction:

Boundary layer cloudiness plays several important roles in the energy budget of the earth. Low level stratocumulus are highly reflective clouds which reduce the net incoming short-wave radiation at the earth's surface. Climatically, the transition to a small area fraction of scattered cumulus clouds occurs as the air flows over warmer water. Although these clouds reflect less sunlight, they still play an important role in the boundary layer equilibrium by transporting water vapor upwards, and enhancing the surface evaporation (Betts, 1986; Betts and Ridgway, 1989). The First ISCCP (International Satellite Cloud Climatology Project) Regional Experiment (FIRE) included a marine stratocumulus experiment off the southern California coast from June 29 to July 19, 1987 (Randall et al, 1984; Albrecht et al, 1988). Among the objectives of this experiment were to study the controls on fractional cloudiness, and to assess the role of cloud-top entrainment instability, CTEI, (Randall, 1980; Deardorff, 1980) and mesoscale structure in determining cloud type.

The focus of this paper is one research day, July 7, 1987, when coordinated aircraft missions were flown by four research aircraft, centered on a Landsat scene at 1830 UTC . The remarkable feature of this Landsat scene (see other papers for photo) is the transition from a clear sky in the west though broken cumulus to solid stratocumulus in the east. In this paper, we analyze the dynamic and thermodynamic structure of this transition in cloudiness using data from the NCAR Electra. By averaging the aircraft data, we shall document the internal structure of the different cloud regimes, and show that the transition between broken cumulus and stratocumulus is associated with a change in structure with respect to the CTEI condition. However, this results not from sea surface temperature changes, but mostly from a transition in the air above the inversion, and the breakup appears to be at a structure on the unstable side of the wet virtual adiabat.

2)   Data Collection and Processing

The flight plan for the Electra (Kloessel et al (1988)), and the data processing is discussed in the extended paper.

a) Averaging of Data into Cloudiness Regimes

The boundary between the cumulus and stratocumulus regimes was moving slowly eastward throughout the time of the Electra

flight. We used observer's notes and the lidar on the aircraft to give an estimate of the mean velocity of the boundary of $3ms^{-1}$. Four regions were identified according to the observed cloudiness which we will refer to as Clear, Cumulus, Broken and Stratocumulus. Clear refers to the far western area where no clouds were present. Only a small fraction of the flight time was spent in this area. Cumulus refers to the region where small puffs of cumulus clouds were visible, but before the clouds developed into larger cells. Broken refers to the transition region between the Cumulus and Stratocumulus where the fractional cloudiness varied between 30% and 75%. Stratocumulus refers to the region towards the west where few holes appeared between clouds and the boundary layer was almost overcast. Approximately equal flight time was spend in the last three regions.

We computed the saturation level quantities of equivalent potential temperature, liquid water potential temperature, and total water mixing ratio and averaged the data of the main east-west flight legs and profile runs in pressure interval bins of 5 hPa for the four cloudiness regimes.

b) Determination of sea surface pressure and temperature

We attempted to compute the sea surface pressure by averaging the sea surface pressure values on the NCAR-Electra aircraft tapes. Inconsistent results were found when different flight legs and levels were compared, with variations of as much as 3 hPa between flight legs means. However horizontal pressure gradients showed consistently an approximately 1.2 hPa decrease in pressure from east to west over a 1 degree longitude interval. We also extrapolated the pressure versus radar altitude plot to the surface, but this surface pressure extrapolation suffers from an uncertainty of 1-2 hPa. We decided to retain the gradients in average sea surface pressure, and use a mean sea surface presure of 1016 hPa consistent with surface synoptic charts. For the sea surface temperature we used the radiometric temperature from the downward looking radiometer corrected for sea surface emission of sky radiation. A necessary estimate of the sky radiation was available from the upward looking radiometer.

3) Results

a) Horizontal gradients and fluxes near the surface.

Fig. 1 shows the west-east cross-section of θ for the sea surface and the average of the two runs at 1010mb. This average was generated by binning the data in 0.05 longitude intervals. To the west in the cumulus and clear regions there is a positive sea-air θ difference, while under the stratocumulus there is a reversal because of the large drop of SST. We computed the surface sensible and latent heat fluxes using the bulk aerodynamic method. Wind-speeds are much higher on the stratocumulus side. We used a constant transfer coefficient of 1.10^{-3}, estimated from Stage and Businger (1981). We compared these bulk fluxes with those measured with the gust-probe system on the Electra (Albrecht, 1989, personal

communication), and found good agreement, considering the number of independent measurements being combined, the residual uncertainties in the sea surface pressure, and our corrections to the Electra temperature and dewpoint observations. The surface latent heat flux decreases across the cumulus-stratocumulus transition, and the surface sensible heat flux falls to near zero or becomes negative.

b) Thermodynamic Profiles

Fig. 2 has four panels showing the average vertical profiles of potential temperature and dewpoint (as a potential temperature) through the BL. Several features can be seen clearly. With the transition from cloud free to stratocumulus regimes (panels (a) to (d)). The BL deepens and, as would be expected, becomes moister until it is saturated. The inversion lifts but becomes stronger. The thermodynamic structure above the inversion shows dramatic differences. There is a tongue of very dry air immediately above the clear region, and this is capped by a moist layer above. The dry tongue disappears with the transition to stratocumulus, and so does the moist layer.

c) Conserved Variable Diagrams

Fig. 3 shows the four thermodynamic profiles on a conserved variable plot of saturation potential temperature, θ^* against total water q^* (Boers and Betts, 1988). Below cloud-base one can see a mixing line profile (Betts, 1982) nearly parallel to the dry virtual adiabat as found by Betts and Albrecht (1987). Above cloud-base and through the inversion, a linear mixing profile with a characteristic slope can be seen. The wet virtual adiabat $\theta_{ev}^* = 310K$ is shown. We see that because of the relatively cool and dry tongue of air above the cloud-free and cumulus CBL's, the mixing line profile through the CBL is very unstable to the wet virtual adiabat in Figs. 3a, 3b. However, the profile through the stratocumulus, and overlying inversion is close to neutral with respect to a wet virtual adiabat. The wet virtual adiabat represents the stability criteria (Betts, 1983) for cloud-top entrainment instability (CTEI), which was suggested as one mechanism for the breakup of stratocumulus by the unstable downward mixing of inversion level air (Randall, 1980; Deardorff, 1980). There has been considerable discussion as to whether CTEI is a sufficient condition for the breakup of stratocumulus (Hanson, 1984, Albrecht et al, 1985; Randall, 1984; Rogers and Telford, 1986; Kuo and Schubert, 1988; Siems et al, 1989 and others). Fig. 3 suggests that CTEI is an important reference process associated with the transition between cumulus and stratocumulus boundary layers, because the mixing line profile through the cumulus layer is very unstable to CTEI whereas through the stratocumulus, it is nearly neutral (albeit slightly unstable). At this time near local noon the stratocumulus does appear to be thinning through the rise of cloud base as it is strongly destabilized by radiative cooling at cloud-top and warming at cloud-base. In this case the highly unstable thermodynamic structure on the cumulus side arises from

the relatively cool layer above the inversion, not from the modest increase in SST, or a large change in mixing ratio above the inversion.

4. Discussion and Conclusions

The transition in structure associated with this transition in cloudiness from a clear sky through tiny cumulus, broken stratocumulus to a solid stratocumulus deck appears to be associated with a large change in the slope of the mixing line. Above the cumulus, the inversion is lower but much weaker in strength and the air above still quite dry, so that the mixing line through the cloud layer is very unstable to the wet virtual adiabat: the criterion for CTEI. Above the stratocumulus, the much stronger inversion gives rise to a mixing line which is only marginally unstable to the CTEI criterion, apparently not enough to break up the solid cloud layer in the face of mixing driven by radiative destabilization and shear generation at the surface. The figures show a clear progression from the clear air, where the mixing down of very dry air ($\approx$ 2gKg^{-1}) appears to be sufficient to prevent any cumulus from forming, to the cumulus regime. Likewise the transition region shows an intermediate thermodynamic structure between cumulus and stratocumulus. From the thermodynamic structure of the broken stratocumulus we can make an estimate (if we ignore all advective effects and assume local equilibrium) of the critical mixing line slope for the formation or breakup of the stratocumulus. Expressed in terms of the slope of the wet adiabat, we obtain

$$(\partial\theta/\partial p)_{crit} \approx 0.7 \; r_w$$

This is more unstable than the wet virtual adiabat which has a slope of 0.9 r_v. There is also some indication in this data that the stratocumulus layer partly uncouples near local noon as has been suggested by Nicholls (1984), and seen in the FIRE data (eg. Betts (1989). The stratocumulus cloud-base as determined by lidar rises 10mb during the flight pattern (2.5 hrs), while the LCL of the low level air descends about 10mb during the same time.

REFERENCES:

Albrecht, B. A., R. Penc, and W. Schubert, 1985: An observational study of cloud-topped mixed layers. J. Atmos. Sci., 42, 800-822.

Albrecht B.A., D.A. Randall and S. Nicholls; 1988: Observations of marine stratocumulus during FIRE. Bull. Amer. Meteor. Soc. 69, 618-626.

Betts, A. K., 1982: Saturation Point Analysis of Moist Convective Overturning. J. Atmos. Sci., 39, 1484-1505.

Betts, A.K., 1983: Thermodynamics of mixed stratocumulus layers: saturation point budgets. J. Atmos. Sci., 40, 2655-2670.

Betts, A. K., 1986: A new convective adjustment scheme. Part I:Observational and theoretical basis. Quart. J. Roy. Meteor. Soc., 112, 677-692.

Betts, A.K. 1989: Diurnal variation of California coastal stratocumulus from two days of boundary layer soundings.

Tellus, 41A, (in press).

Betts, A. K., and B. A. Albrecht, 1987: Conserved variable analysis of boundary layer thermodynamic structure over the tropical oceans. J. Atmos. Sci., 44, 83-99.

Betts, A.K. and W. L. Ridgway, 1989: Climatic equilibrium of the atmospheric convective boundary layer over a tropical ocean. J. Atmos. Sci., 46, (Aug)

Boers, R., and A. K. Betts, 1988: Saturation point structure of marine stratocumulus clouds. J. Atmos. Sci. 45, 1157-1175.

Deardorff, J.W., 1980: Cloud-top entrainment instability. J. Atmos. Sci., 37, 131-147.

Hanson, H. 1984: On mixed layer modelling of the stratocumulus topped marine boundary layer. J. Atmos. Sci., 41, 1226-1236.

Kloessel, K.A., B.A. Albrecht, and D.P. Wylie, 1988: FIRE Marine stratocumulus observations Summary of operations and synoptic conditions. FIRE Tech.Report No.1. Dept. of Meteor., Penn State Univ., Univ. Park, PA 16802. 191 pp.

Kuo, H-C, and W.H. Schubert, 1988: Stability of cloud-topped boundary layers. Quart. J. Meteor. Soc., 114, 887-916.

Lilly, D. K., 1968: Models of cloud-topped mixed layers under a strong inversion. Quart. J. Roy. Meteor. Soc., 94, 292-309.

Nicholls, S. 1984: The dynamics of stratocumulus: Aircraft observations and comparisons with a mixed layer model. Quart. J. Roy. Meteor. Soc., 110, 783-820.

Randall, D.A., 1980: Conditional instability of the first kind upside-down. J. Atmos. Sci., 37, 125-130.

Randall, D. A., 1984: Stratocumulus cloud deepening through entrainment. Tellus, 36A, 446-457.

Randall, D.A., J.A. Coakley, C.W. Fairall, R.A. Kropflin and D.H. Lenschow, 1984: Outlook for research on subtropical marine stratform clouds. Bull. Amer. Meteor. Soc., 65, 1290-1301.

Rogers, D., and J.W. Telford, 1986: Metastable stratustops. Quart. J. Roy. Meteor. Soc., 112, 481-500.

Schubert, W.H., J. S. Wakefield, E. J. Steiner, and S. K. Cox, 1979: Marine stratocumulus convection. Part I: Governing equations and horizontally homogeneous solutions. J. Atmos. Sci. 36 1286-1307.

Stage, S. A. and J. A. Businger, 1981: A model for entrainment into a cloud-topped boundary layer. Part I: Model description and application to a cold air outbreak. J. Atmos. Sci., 38, 2213-2229.

Siems, S.T., C.S. Bretherton, M.B. Baker, S. Shy, and R.T. Breidenthal, 1989: Buoyancy reversal and cloud-top entrainment instability. Submitted to Quart. J. Roy. Meteor. Soc.
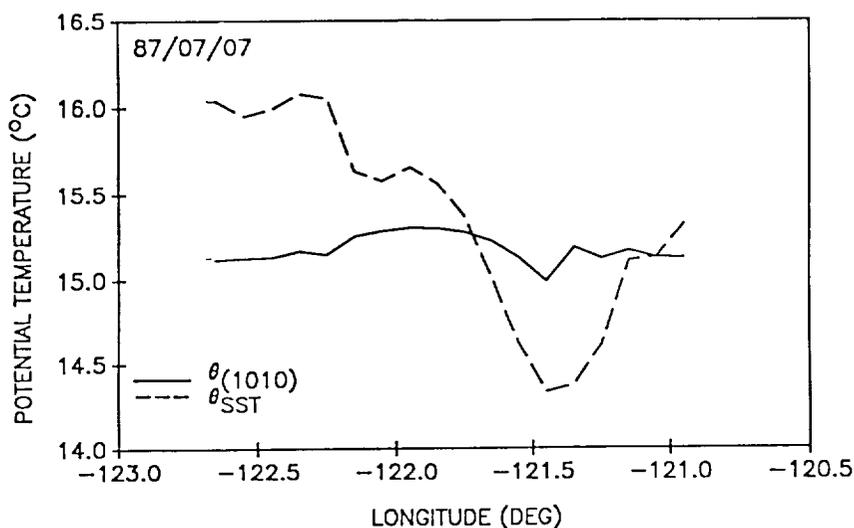
Fig. 1   Cross-section of θ for sea surface and 1010mb.

87/07/07 CLEAR REGION

p (hPa)

θ, θ_d (°C)

87/07/07 CUMULUS REGIME

p (hPa)

θ, θ_d (°C)

87/07/07 BROKEN REGION

p (hPa)

θ, θ_d (°C)

87/07/07 STRATOCU REGION

p (hPa)

θ, θ_d (°C)
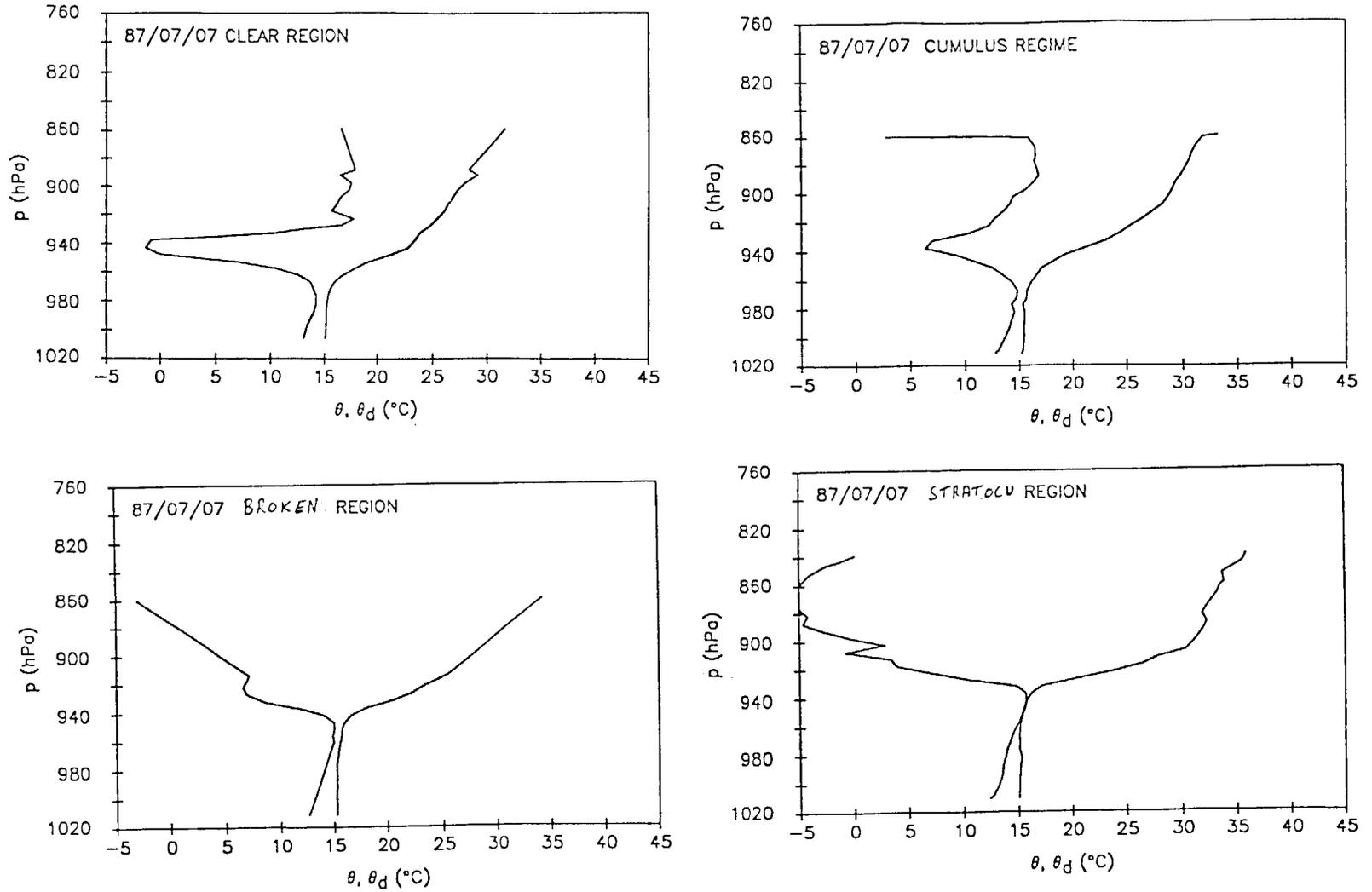
Fig. 2   Mean thermodynamic profiles for four regimes: clear, cumulus, broken, stratocumulus.
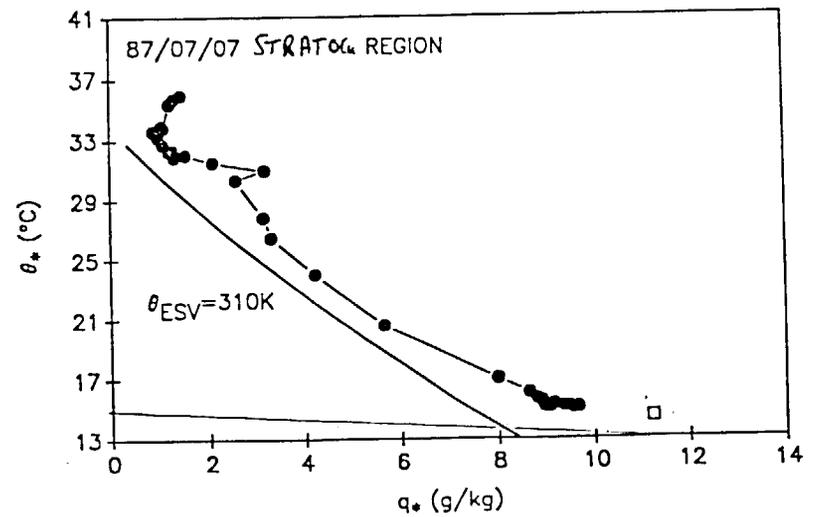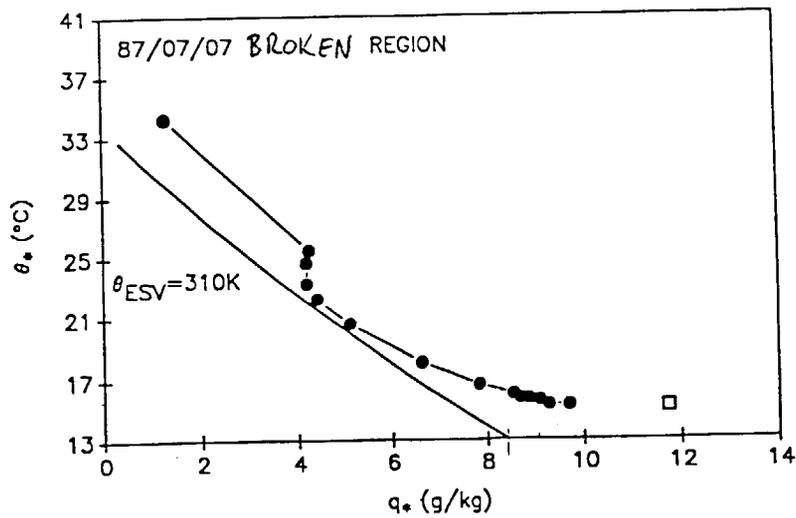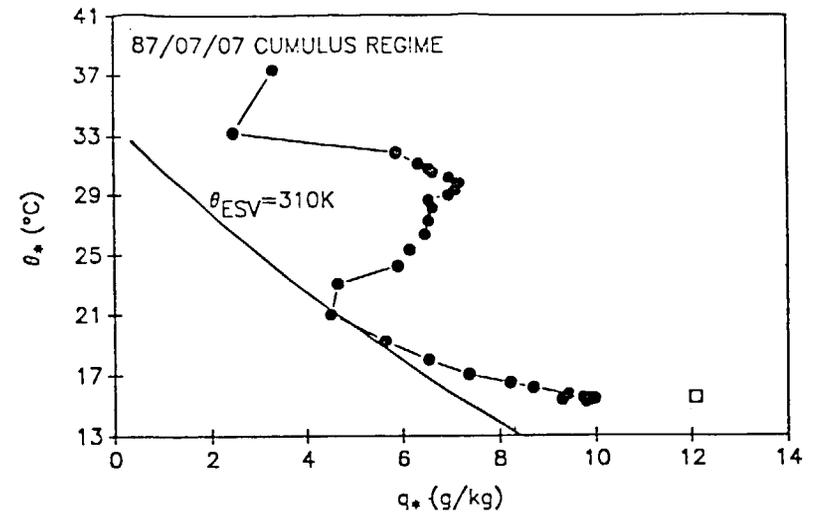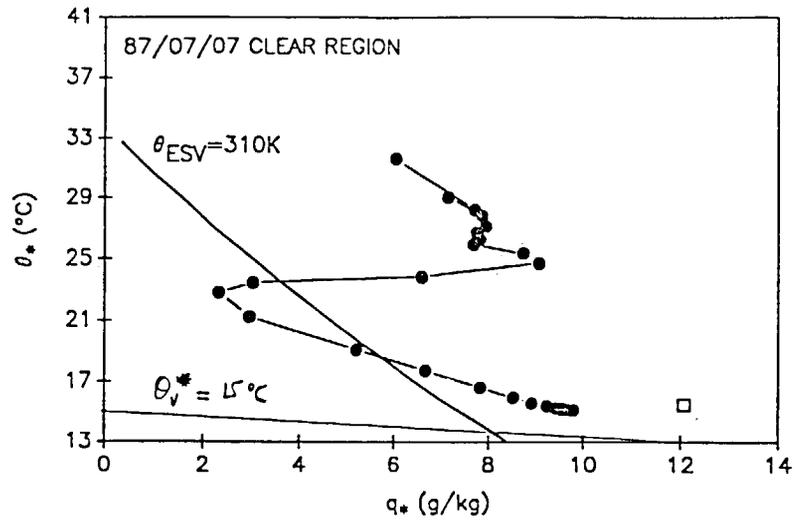
Fig. 3   Conserved variable plots ($\theta^{\dagger}$, $q^{\dagger}$) showing profiles for four regimes.